Preliminary Progress in Establishing Motion Fidelity Requirements for Maritime Rotorcraft Flight Simulators

Wajih A Memon, Mark D White and Ieuan Owen
University of Liverpool
Liverpool, United Kingdom

Sophie Robinson
Kopter Group AG
Zürich Area, Switzerland

ABSTRACT

The research presented in this paper is part of a project underway at the University of Liverpool (UoL) which aims to develop overall simulation fidelity requirements for maritime rotorcraft flight simulators. This requires a structured examination of individual Modelling and Simulation (M&S) elements, such as motion and visual cues, flight dynamics model and ship airwake integration. The paper reports the initial results of motion cueing research that has been conducted to assess and optimise the motion drive laws and determine high fidelity motion cueing for simulated shipboard operations. To do this, an objective technique, Vestibular Motion Perception Error (VMPE), has been developed. The technique was utilised to optimise the motion cues in UoL's Heliflight-R simulator for a simulated helicopter landing on an aircraft carrier in a turbulent environment. Four motion tuning sets were derived offline and experimentally tested. Results show the influence of different motion cues and airwake conditions on the pilot's overall self-motion perception, control strategy and task performance. It was found that high-fidelity motion cueing becomes more desirable for the pilot at higher airwake wind conditions, for which an 'Optimised' motion setting was obtained using the new technique, than at lower airwake turbulence conditions.

NOTATION

F_{AA} = Aircraft specific force vector at aircraft's c.g. (m/s^2).
F_{A_Per}, F_{S_Per} = Perceived specific force in aircraft and simulator (rad/s).
F_{RC} = Aircraft specific force vector at the rotational centre of the simulator (m/s^2).
F_{S_P} = Simulator specific force vector at pilot vestibular centre (m/s^2).
F_{S_RC} = Simulator specific force vector at rotational centre of the simulator (m/s^2).
$NRMSE_{VMPE\_F}$ = Normalized RMSE of the specific force perceived b/w aircraft and simulator.
$NRMSE_{VMPE\_\omega}$ = Normalized RMSE of the angular rate perceived b/w aircraft and simulator.
$RMSE_{VMPE\_F}$ = RMSE of the specific force perceived (m/s^2) b/w aircraft and simulator.
$RMSE_{VMPE\_\omega}$ = RMSE of the angular rate perceived in (deg/s) b/w aircraft and simulator.
$VMPE_{NRMSE\text{-}MTS}$ = Total VMPE measure of motion tuning set (%).
$VMPE_{RMSE\text{-}MTS\text{-}F}$ = Total VMPE measure of a motion tuning set for the translational channel (m/sec^2).
$VMPE_{RMSE\text{-}MTS\text{-}\omega}$ = Total VMPE measure of the motion tuning set for the rotational channel (deg/sec).

a_x, a_y, a_z = Aircraft linear accelerations (m/s^2).
a_{xs}, a_{ys}, a_{zs} = Simulator linear acceleration demands (m/s^2).
f-per = Perceived specific forces (m/s^2).
f_x, f_y, f_z = Aircraft specific forces (m/s^2).
f_{xs}, f_{ys}, f_{zs} = Simulator specific forces (m/s^2).
k = HP and LP filter gain.
p,q,r = Angular velocities of the aircraft (deg/s).
u,v,w = Aircraft linear velocities (m/s).
u_s, v_s, w_s = Simulator linear velocity demands (m/s).
x,y,z = Linear aircraft displacements (ft).

ω_n = HP and LP filter washout or break frequency.
ω_{AA} = Aircraft angular velocity vector (rad/s).
$\omega_{A\_Per}, \omega_{S\_Per}$ = Perceived angular rate in aircraft and simulator (rad/s).
ω-per = Perceived angular velocity (rad/s).
ω_s = Simulator angular velocity vector (rad/s).
ϕ, Θ, ψ = Aircraft angular displacement (rad).
ϕ_s, Θ_s, ψ_s = Simulator angular displacement (rad).

INTRODUCTION

The United Kingdom's Royal Navy and Royal Fleet Auxiliary regularly perform helicopter launch and recovery operations to and from their ships. These operations are carried out in challenging conditions which are unique to the maritime environment. The combination of a confined ship deck landing space for launch and recovery of helicopters, together with irregular ship motion, sea spray and unsteady airflow over and around the ship's deck and superstructure, produce a high risk and operational demand to/on the helicopter, ship and crew. Together, these elements form the Helicopter Ship Dynamic Interface (HSDI) environment (Ref. 1) (Figure 1).

Figure 1: Helicopter Ship Dynamic Interface Environment

To determine the limitations of the safe operability of helicopters to/from ships, a safety envelope is constructed through First of Class Flight Trials (FOCFTs) to determine Ship Helicopter Operating Limits (SHOLs) for every in-service combination of helicopters and ships. The SHOL details the safe conditions for launch and recovery operations (Ref. 2). FOCFTs are performed at sea and are inevitably very expensive and can typically take weeks to construct a full SHOL envelope. Often the full range of wind and sea conditions (e.g. wind magnitudes and azimuths, sea states) may not be available during at-sea trials, resulting in the development of a conservative SHOL (Ref. 3). An example of a SHOL diagram for a Royal Navy helicopter operating to/from a frigate is shown in Figure 2 (for winds from ±90° from ahead). The SHOL consists of radial and circumferential lines of wind azimuth and magnitude, respectively, representing the Wind Over Deck (WOD) condition at the deck landing spot. The SHOL limit is shown as a bold black line, and the area inside this boundary indicates the combinations of wind speed/direction that are safe to land in.

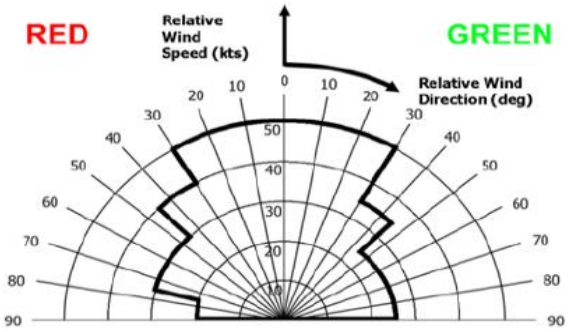

Figure 2: Typical SHOL Diagram

For the reasons detailed above, M&S of the HSDI environment is being developed in flight simulators to mitigate these operational and meteorological risks, making SHOL testing safer, quicker, and more cost-effective (Refs. 4-6). Whilst it is not trying to fully replace at-sea testing, M&S aims to inform the key test points or "Hot Spots" of uncertainty to test at sea. However, the reliability of this support depends upon the identification of the fidelity requirements of the HSDI M&S elements integrated into the flight simulation environment, such as the motion and visual cueing, the flight dynamics model and the integration of unsteady airflow to represent the ship's airwake (Ref. 5), which itself is a significant technical challenge.

Attempts have been made to assess the fidelity of research and maritime engineering rotorcraft simulators, e.g. Joint Shipboard Helicopter Integration Process (JSHIP) project, which examined the viability of the use of flight simulators in defining the shipboard operational limitations (Ref. 5). Moreover, helicopter-ship research undertaken at the UoL has examined the effect of motion, visual and airwake fidelity on overall simulation fidelity, pilot workload, task performance and subjective assessment (Refs. 7-9). Research has been undertaken to quantify the overall fidelity of rotorcraft simulations (Refs. 10, 11), for its use in design, development, training and qualification. Current simulator qualification standards, CS-FSTD-H (Ref. 12) and 14 CFR Part 60 (Ref. 13) provide guidelines for the assessment of the component fidelity of civil training simulators which primarily

defines the acceptable match between aircraft and simulators to be deemed fit for training purposes. However, even if a simulator is quantified to have the highest level of component fidelity, it might still not have a good overall simulation fidelity which may be defined as "the simulator that induces the pilot to behave in a similar way as in the real aircraft" (Refs. 14, 15).

Whilst existing literature provides qualification methods, especially for the civil training simulators, these are not necessarily directly applicable to research simulators. A standardized guideline to quantify and qualify the overall fidelity of research and engineering simulators is a challenge which is yet to be fully addressed (Ref. 16).

UoL's Flight Science and Technology research group operates and uses a fully reconfigurable research simulator, Heliflight-R, for the purpose of analysing the flight handling qualities, pilot workload assessment, flight model development and simulation fidelity for land-based and HSDI operations (Ref. 16). It has been at the forefront of the research to develop a high-fidelity HSDI simulation environment. (Refs. 3, 8).

The research presented is part of a project jointly funded by QinetiQ and Dstl, which aims to achieve the following objective, "To undertake a structured examination of the M&S elements of the HSDI simulation environment to develop a new robust simulation fidelity matrix to support at sea flight trials". The examination includes the analysis, evaluation, and improvement of the visual cues, motion cues, airwake integration process, and vehicle modelling. Moreover, it will develop a robust simulation fidelity matrix which will help to define the requirements for components of the HSDI simulation that are needed to inform the "real-world" SHOL trials with a reliable level of confidence. Figure 3 shows the HSDI M&S elements integrated into the Heliflight-R simulator.

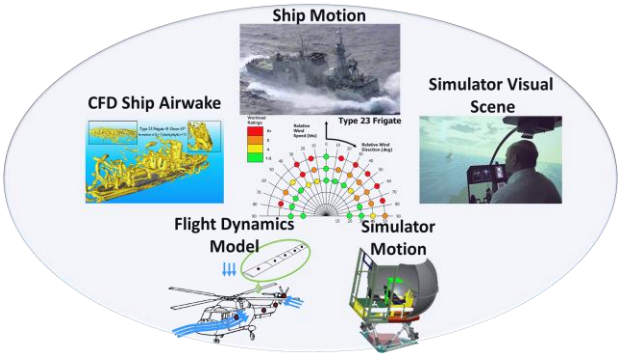

Figure 3: HSDI Modelling and Simulation Elements

Among the core elements of the HSDI M&S environment, vestibular motion cueing is the initial focus of the project.

MOTION CUEING: PRINCIPLE AND BACKGROUND

Motion cueing remains an important area of research due to a gap in existing knowledge regarding its fidelity requirements, particularly in the HSDI environment. There currently is no robust tool available to efficiently tune the motion platform to allow the pilot to perceive "High-fidelity" motion cues in the HSDI environment despite significant research in land-based tasks (Refs. 17-20). These studies have shown that motion cueing requirements are task-specific which means that for each task the simulator's motion must be specially tuned based on the dominant axis and the requirements of the task (Ref. 17). Therefore, it is difficult to obtain a single motion setting which can be universally used in all the different tasks providing sufficient motion cues to the pilot. The factors which affect the pilot's motion perception are determined by the motion platform hardware and configuration of the Motion Drive Algorithm (MDA) (Ref. 17). The focus of this research is based on tuning the MDA to optimise the vestibular motion cues for a deck landing task performed in rotorcraft flight simulator.

Motion cues in a flight simulator are perceived from visual information projected onto the human eye (i.e. visual motion cues also known as vection) and from the simulator's motion platform movement detected by the vestibular system in the human ear and proprioceptive/kinaesthetic cueing (Ref. 21). The vestibular system consists of two parts; the Semi-Circular Canals (SCC) and the Otoliths (Oto). The 'SCC' acts as a damped angular accelerometer which senses the angular rates and 'Oto' senses the specific forces (gravitational less linear accelerations) obtained at the pilot Vestibular Centre (VC) (Refs. 16, 21, 22).

Motion cues obtained from the simulator platform's physical movement should be complementary to the motion cues obtained from the visual projection system. Poor synchronisation of the stimulation and response of optical flow and inertial motion can

result in inaccurate vestibular and/or visual motion cues, leading to vague overall self-motion perception and compromised subjective ratings and task performance from the pilots during piloted simulation flight trials (Ref. 23).

The motion demands of the flight simulator are produced by a MDA, which contains washout filters that tailor the simulator's motion response. There are typically three types of MDAs used in simulators: classical motion cueing algorithm, adaptive washout algorithm and optimal higher order motion drive algorithm. The most commonly used MDA is a Classical Washout Algorithm (CWA) proposed by Reid and Nahon (Ref. 24), shown in Figure 4. It allows easy analysis of the filter settings and its response due to its linear filtering technique. The CWA has been shown to achieve reasonably good results compared to the other two MDAs (Ref. 25).

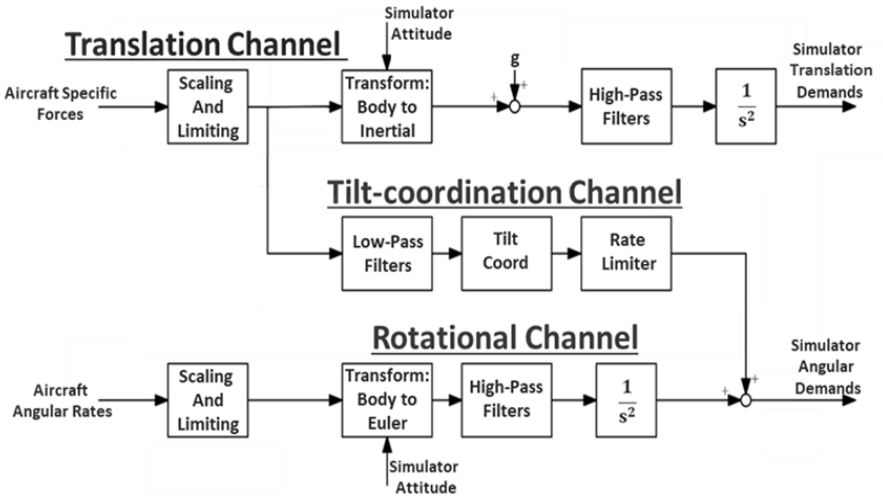

Figure 4: Classical Washout Algorithm (CWA)

The CWA captures the aircraft body states and attenuates them to produce simulator motion demands which are then sent to the motion platform hardware. A CWA consists of three channels: translational, rotational and tilt-coordination. Translational and rotational channels each contain three high-pass (HP) washout filters and the tilt-coordination channel contains two low-pass (LP) washout filters. The quantity and the quality of the motion attenuation depend upon the tuning of the HP and LP filter coefficients: gains 'k' and washout or break frequencies 'ω_n', which alter the motion base's response, hence changing overall behaviour of the motion. Altogether, there are sixteen filter coefficients. The collection of these coefficients in all six axes forms a Motion Tuning Set (MTS).

The inputs to the CWA are aircraft specific forces (gravitation less force per unit mass acting on the aircraft 'F_{AA}') and aircraft angular rates 'ω_{AA}', as shown in Figure 4. The HP filter allows the high-frequency signals to pass through while it blocks the low-frequency signals, which in the translational and rotational channel are sustained accelerations that would result in simulator actuator hitting its excursion limits (motion envelope limits). The HP filter in the translational and rotational channel is a 3rd order filter which provides the washout characteristics that will result in returning the motion of the platform to its neutral position, after an initial onset acceleration (Ref. 19). The LP filter in the tilt-coordination channel allows the low-frequency signals (sustained linear accelerations) to pass through it, which produces the angular displacement of the simulator providing a linear displacement sensation to the pilot. However, it is important that the pilot does not sense that the linear acceleration sensation is provided via angular displacement of the simulator. Therefore, the channel is rate limited at between 2-3 deg/sec to keep the angular rate below human perception threshold (Ref. 19). The main purpose of the tilt-coordination is to provide a linear displacement sensation which cannot be provided directly due to constrained simulator motion envelope and makes use of the Somatogravic illusion (Ref. 26).

Several studies have been conducted on motion cueing optimisation for flight and driving simulators. Existing literature on motion cueing has proposed different strategies for its assessment and optimisation potentially using frequency domain techniques (e.g. Sinacori criteria) (Ref. 31), pilot subjective opinion tuning technique which is a non-systematic time-consuming approach using pilot-in-the-loop simulations (Refs. 16, 17) and genetic algorithms (GA) using fitness functions (Refs. 27, 28).

A method for objective motion fidelity assessment of the flight simulators, i.e. Objective Motion Cueing Test (OMCT) has also been proposed in ICAO-9625 (Ref. 12), which defines the requirement for the completion of robotic tests by the flight simulators. It was published originally for the fixed-wing aircraft simulators and is performed in the absence of the pilot and

real-world tasks. An OMCT was conducted on UoL's Heliflight-R simulator by Jones et al. (Ref. 18), which showed a mismatch between the obtained test results and OMCT fidelity acceptance boundaries, suggesting further rotorcraft related motion fidelity research is required. Piloted simulations were also conducted for motion cueing optimisation in ADS-33E-PRF (Ref. 34) and ADS-33 (Maritime) (Ref. 35) land-based tasks and the results showed a disagreement between subjective motion fidelity assessments and the current OMCT acceptance regions.

Recently, automatic GA based motion tuning techniques have been used for motion parameter optimisation. The GA is a stochastic algorithm which uses a heuristic approach to solve motion optimisation problem by minimising a fitness function. Sergio et al. (Ref. 26) demonstrated the application of a GA for determining the best motion cues using a simulated virtual motion platform. Asadi et al. (Ref. 27) introduced an optimal MDA for driving simulators based on a GA approach and non-linear filtering. Whilst Jones (Refs. 18, 28) has used a GA to enhance the motion cues in rotorcraft simulators and has conducted flight trial experiments to demonstrate a correlation between GA results and subjective pilot assessments, which show encouraging results.

However, most of these motion optimisation studies have primarily focused upon single/multi-axis (not full-axis) land-based tasks, typically undertaken in the absence of factors such as an unsteady airwake and landing spot movement, which are significant fidelity elements in the HSDI environment (Refs. 1-6). In HSDI operations, unsteady aerodynamic forces act upon the helicopter due to the airwake produced by the wind over and around the ship's deck and superstructure, which the pilot needs to compensate for to perform the required landing task successfully. The inclusion of such effects has not been fully examined in the literature related to motion fidelity. Therefore, the results obtained from the land-based research cannot be directly transferred to the full-axis maritime operations. Further research is required to assess the motion fidelity characteristics and fidelity requirements of simulator motion drive laws for HSDI applications.

This paper reports the initial results of motion cueing research that has been conducted to optimise motion drive laws for HSDI operations. To objectively assess and optimise the motion cues and determine high fidelity motion cueing for HSDI operations, an offline heuristic approach, reported as Vestibular Motion Perception Error (VMPE), has been developed based on a motion perception error minimisation strategy. VMPE is the measure of the deviation between vestibular motion perceived by the pilot in the simulator and the simulated aircraft, which is minimised for the purpose of motion cueing optimisation using a trade-off MDA parameter tuning strategy.

Motion Platform: Heliflight-R

Heliflight-R simulator is a fully reconfigurable research rotorcraft flight simulator at the University of Liverpool, (Figure 5); acceptance and commissioning of the simulator was completed in 2008 (Ref. 16). The simulator has been utilised for a wide range of research projects and for undergraduate Aerospace Engineering research and teaching activities (Ref. 29). It consists of a 12ft diameter visual dome mounted on a 6-DOF short stroke Moog hexapod motion system. The simulator uses three high-resolution 2560x1600 projectors providing a field of view horizontally of 220^{o} and vertically of 70^{o}.

Figure 5: UoL's Heliflight-R Simulator (foreground)

The limits of the Heliflight-R simulator motion platform are shown in Table 1 (Ref. 16).

Table 1: Heliflight-R Simulator Motion Envelope.

Axis	Displacement	Velocity	Acceleration
Pitch	-23.3º/25.6º	±34º/s	300º/s^2
Roll	±23.2º	±35º/s	300º/s^2
Yaw	±24.3º	±36º/s	500º/s^2
Heave	±0.39m	±0.7m/s	±1.02g
Surge	-0.46/0.57m	± 0.7m/s	±0.71g
Sway	±0.47m	±0.5m/s	±0.71g

MOTION OPTIMISATION: METHODOLOGY

The motion assessment and optimisation approach proposed in this study is based on the concept of minimising the estimated error between the vestibular motion perceived by the pilot in the flight simulator and the simulated aircraft by tuning the CWA parameters to produce an optimal motion platform setting. Since flight simulators, due to their physical limitations, cannot reproduce the sustained accelerations of the aircraft completely, they can only provide the illusion of real aircraft motion to the simulator pilot. Therefore, it is important to tune the system with a formal and rational evaluation methodology which provides a reliable measure of the simulator motion fidelity. For the initial assessment of the proposed model and its utilisation for offline motion optimisation for the HSDI operations, a simulated CWA was developed in Matlab/Simulink and validated with a simulator trial. This allowed testing of a large number of MTSs during the course of the optimisation process to achieve the desired motion setting (i.e. MTS) without using actual simulator hardware.

The model for the proposed VMPE technique was developed and incorporated within a CWA developed in Simulink, as shown in Figure 6. The combined system consists of four sub-systems: CWA, Actuator kinematics, Motion centroid transformation and Vestibular motion perception model. Altogether it undergoes a five-step process for determining the optimal MTS for the desired task. The input to the system is same as the input to the MDA (i.e. the aircraft translational accelerations and angular velocities) extracted from a Heliflight-R piloted simulation flight trial database and the output from the system is the MTS with the VMPE measure value. The system has a dedicated simulator actuator excursion limit indicator which helps to derive a MTS that constrains the Heliflight-R simulator platform into its motion envelope specified in Table 1.

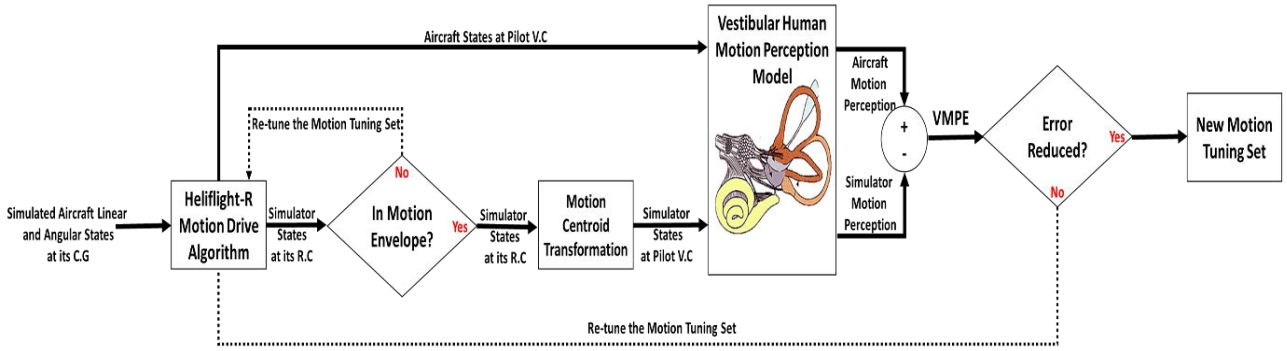

Figure 6: Vestibular Motion Perception Error (VMPE) Technique Architecture

The process begins with capturing the simulated helicopter body states obtained from a helicopter model and calculates the simulator inertial motion demands at its Rotational Centre (RC) using the CWA. The aircraft linear body accelerations are first transformed into the specific forces F_{AA} (gravitation less force per unit mass acting on the aircraft, in m/sec^2) at its c.g. using Eqn. 1, (Ref. 31). These specific forces, along with the angular velocity of the aircraft, are input to the Heliflight-R MDA, as shown in Figure 4.

$$F_{AA} = \begin{pmatrix} f_{xAA} \\ f_{yAA} \\ f_{zAA} \end{pmatrix} = \begin{pmatrix} a_x \\ a_y \\ a_z \end{pmatrix} - \begin{pmatrix} g_x \\ g_y \\ g_z \end{pmatrix} = \begin{pmatrix} \dot{u} \\ \dot{v} \\ \dot{w} \end{pmatrix} - \begin{pmatrix} r \\ p \\ q \end{pmatrix} \begin{pmatrix} v \\ w \\ u \end{pmatrix} + \begin{pmatrix} q \\ r \\ p \end{pmatrix} \begin{pmatrix} w \\ u \\ v \end{pmatrix} - g \begin{pmatrix} -sin\Theta \\ sin\Phi cos\Theta \\ cos\Phi cos\Theta \end{pmatrix} \quad (1)$$

The aircraft specific forces, F_{AA}, before being passed through the washout HP and LP filters, are transformed to the location which physically corresponds to the motion centre of the Heliflight-R simulator 'RC' using Eqn. 2, (see Figure 7). The specific forces at this point are denoted as F_{RC}.

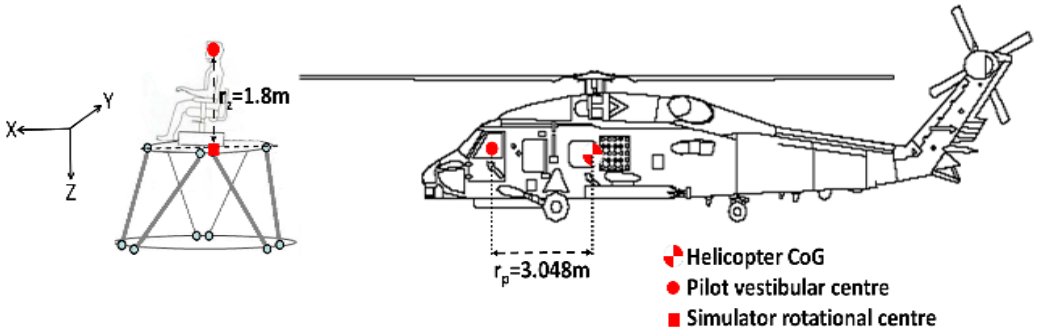

Figure 7: Motion Centroid Transformation between Helicopter and Simulator (SH-60 configuration)

$$F_{RC} = F_{AA} + \omega_{AA} \times (\omega_{AA} \times R) + \omega'_{AA} \times R \tag{2}$$

where 'ω_{AA}' is the aircraft angular velocity vector and 'R' is the position vector between aircraft's c.g. and simulator's RC. These forces are scaled and limited first and then passed through the washout filters.

The next step is to determine the aircraft and simulator states at the VC of the human pilot (i.e. at the pilot's ear). This is required because the human senses the whole body motion through the vestibular system present in the ear, which is approximately 1.8m above the RC of the Heliflight-R simulator denoted by 'r_z' and 3.048m ahead of the c.g. of the aircraft denoted by 'r_p', in Figure 7 (Ref. 19). Eqn. 3 is used to obtain the aircraft specific forces at the pilot position:

$$F_{A\_P} = F_{AA} + \omega_{AA} \times (\omega_{AA} \times r_P) + \omega'_{AA} \times r_P \tag{3}$$

To determine the simulator specific forces at the pilot position, firstly, the simulator motion demands obtained at the output of the CWA within the first step are transformed to the specific forces at the RC of the simulator using Eqn. 4.

$$F_{s\_RC} = \begin{pmatrix} f_{xs\_RC} \\ f_{ys\_RC} \\ f_{zs\_RC} \end{pmatrix} = \begin{pmatrix} a_{xs} \\ a_{ys} \\ a_{zs} \end{pmatrix} - \begin{pmatrix} g_{xs} \\ g_{ys} \\ g_{zs} \end{pmatrix} = \begin{pmatrix} \dot{u}_s \\ \dot{v}_s \\ \dot{w}_s \end{pmatrix} - \begin{pmatrix} r_s \\ p_s \\ q_s \end{pmatrix} \begin{pmatrix} v_s \\ w_s \\ u_s \end{pmatrix} + \begin{pmatrix} q_s \\ r_s \\ p_s \end{pmatrix} \begin{pmatrix} w_s \\ u_s \\ v_s \end{pmatrix} - g \begin{pmatrix} -sin\Theta_s \\ sin\Phi_s cos\Theta_s \\ cos\Phi_s cos\Theta_s \end{pmatrix} \tag{4}$$

In Eqn. 4 the accelerations and velocities represent the simulator states in the body frame, whereas Eqn. 1 represents the aircraft states. Following that, the simulator specific forces at the pilot VC in the simulator are calculated using Eqn. 4 in Eqn. 5:

$$F_{s\_P} = F_{s\_RC} + \omega_s \times (\omega_s \times -r_z) + \omega'_s \times -r_z \tag{5}$$

where '$-r_z$' is the position vector from RC of the simulator to the VC of the pilot in the simulator, see figure 7.

Finally, the specific forces at the pilot's VC in the aircraft and simulator are obtained. The angular velocities do not need position transformation since they are independent of the location on the body it is applied at. Care should be taken of the frame of reference (i.e. body frame or inertial frame).

In this step, the perceived specific forces and angular velocities sensed by the pilot's vestibular system in the helicopter and simulator are estimated by utilising the actual specific forces and angular velocities obtained in the previous step. This is achieved using the vestibular system dynamics transfer functions (Eqns. 6 and 7) given by Telban and Cardullo (Ref. 22). Since the vestibular system has two parts: semi-circular canal and otoliths for angular velocity and linear specific force sensation, respectively, two different models are used to simulate the human vestibular sensory dynamics.

A transfer function of the Otoliths which links the perceived specific force output to actual specific force input is given as follows:

$$TF_{OTO}(s) = 0.4 \frac{10s+1}{(0.08s^2+5.016s+1)} \tag{6}$$

A semi-circular canal model transfer function which links perceived angular velocity output to actual angular velocity input is given as follows:

$$TF_{SCC}(s) = 5.73\frac{80s^2}{(458.34s^2+85.73s+1)} \tag{7}$$

The estimated specific force and angular velocity perception in simulated aircraft and simulator are then compared against each other to calculate the VMPE (i.e. motion perception error) between them. The VMPE gives the measure of the motion cueing fidelity in the flight simulator. The measure employed to quantify the VMPE is Root Mean Square Error (RMSE), using the Eqns. 8 and 9:

$$\text{RMSE}_{\text{VMPE\_Fi}} = \sqrt{\frac{\sum_{k=1}^{N}(F_{Ai\_Per}-F_{Si\_Per})^2}{N}} \text{ (m/sec}^2\text{)} \tag{8}$$

$$\text{RMSE}_{\text{VMPE\_}\omega\text{i}} = \sqrt{\frac{\sum_{k=1}^{N}(\omega_{Ai\_Per}-\omega_{Si\_Per})^2}{N}} \text{ (deg/sec)} \tag{9}$$

where 'i' corresponds to the (x, y, z) axis, 'N' is the length of the data vector, 'F_{A_Per}' and 'F_{S_Per}' are perceived specific forces and 'ω_{A_Per}' and 'ω_{S_Per}' are perceived angular velocities, in simulated aircraft and flight simulator. The RMSs of motion perception errors are calculated individually for each axis within each channel (translational and rotational) separately using the above equations and averaged to determine the VMPE for a motion tuning set using Eqns. 10 and 11.

In the cases where the task under examination have dominant motion axes belonging to the same channel, i.e. rotational (pitch, roll and/or yaw) or translational (surge, sway and/or heave), such as in Superslide task, etc., then the VMPE of the MTS can simply be obtained by taking the average of the RMSEs of the dominant axis using Eqns. 10 and 11.

$$\text{VMPE}_{\text{RMSE-MTS-F}} = \frac{\sum_{k=1}^{m}(RMSE_{VMPE\_Fi})}{m} \text{ (m/sec}^2\text{)} \tag{10}$$

$$\text{VMPE}_{\text{RMSE-MTS-}\omega} = \frac{\sum_{k=1}^{m}(RMSE_{VMPE\_\omega i})}{m} \text{ (deg/sec)} \tag{11}$$

where 'm' is the number of dominant axes.

In the cases where the dominant motion axis of the task belong to both rotational and translational channels (e.g. full axis deck landing task) then RMSEs obtained for each axis using Eqns. 8 and 9 are normalized first by the range (maximum value-minimum value) of the perceived motion in the aircraft (i.e. the reference value) and then averaged to obtain the VMPE of the MTS. The normalisation is carried out using the range and not mean because the mean value of the aircraft motion perception is around zero which will result in an unrealistic NRMSE value (Refs. 32, 33). The normalisation is achieved using Eqns. 12 & 13 and finally, the VMPE of the MTS is obtained by averaging the NRMSEs obtained for each axis. NRMSEs can be specified in percentage as shown in Eqn. 14.

$$\text{NRMSE}_{\text{VMPE\_Fi}} = \frac{RMSE_{VMPE\_Fi}}{max(F_{Ai\_Per})-min(F_{Ai\_Per})} \tag{12}$$

$$\text{NRMSE}_{\text{VMPE\_}\omega\text{i}} = \frac{RMSE_{VMPE\_\omega i}}{max(\omega_{Ai\_Per})-min(\omega_{Ai\_Per})} \tag{13}$$

$$\text{VMPE}_{\text{NRMSE-MTS}} = \frac{(NRMSE_{VMPE\_Fx}+NRMSE_{VMPE\_Fy}+NRMSE_{VMPE\_Fz}+NRMSE_{VMPE\_\omega x}+NRMSE_{VMPE\_\omega y}+NRMSE_{VMPE\_\omega z})}{m} \text{ x 100 (\%)} \tag{14}$$

The primary fidelity objective of the simulator has been to provide initial accelerations to the pilot in the simulator which are representative of the real helicopter. Therefore, using this methodology, the purpose of motion optimisation is achieved by minimising the VMPE by tuning the parameters of the CWA filter (k and ω_n) in the channels of interest, while keeping the simulator actuator excursion constrained in its motion envelope (i.e. 0.6m actuator stroke). The application of VMPE is detailed in the next step.

VMPE Application

The VMPE technique was utilised to assess and optimise the motion cueing in the UoL's Heliflight-R simulator. The technique was applied in three phases: Pre-validation, Pre-trial optimisation and Simulated flight trial experiment. In the pre-validation phase, the offline VMPE results were compared and correlated with pilot's subjective assessments obtained from a previous motion-dedicated flight trial experiment conducted in Heliflight-R simulator. In the optimisation phase, the offline VMPE technique was utilised to derive new MTSs for the landings of a SH-60B (Seahawk) FLIGHTLAB helicopter model to the UK's new aircraft carrier, the Queen Elizabeth Class (QEC), at three different airwake conditions (windspeeds of 25, 35 and 45kts in a headwind 'H00' direction) in the Heliflight-R simulator. Finally, a piloted simulation flight trial experiment was conducted for the same QEC deck landing task using the same airwake conditions to examine the motion cueing fidelity and validate the VMPE predictions.

Phase I: Pre-validation

The pre-validation phase consisted of calculating the VMPEs for the MTSs obtained from a land-based piloted simulation motion trial experiment conducted by Jones et al. in the Heliflight-R simulator using a Bell-412 FLIGHTLAB simulated helicopter model. (Ref. 18), which provided single-axis and multi-axis cueing demands. The simulator's motion characteristics were examined in the specific dominant axes of the mission tasks within this experiment as follows.

MTSs tested during two ADS-33E-PRF MTEs (Ref. 34) and a ADS-33 (Maritime) surrogate land-based maritime task (Ref. 35) were acquired from Jones et al.'s experiment, namely the Superslide, Lateral reposition, and Pirouette, tasks. The flight model accelerations needed to calculate VMPEs were available from these tasks. In all these tasks, the dominant axis belongs to the angular channel in which the motion parameter variation was undertaken, while motion filter parameters in other non-dominant axes remained constant. The main idea here was to compare the pattern of the VMPE (objective assessment) estimations with Overall Motion Fidelity Rating (subjective assessment) results obtained from the motion experiment, to assess the viability and correctness of the VMPE technique for offline pre-trial motion assessment and optimisation. The rating scale used to obtain the Overall Motion Fidelity Rating (OMFR) in the flight trial experiment is called the Jones Motion Rating Scale proposed by Jones et al. (Ref. 18), shown in Figure 8.

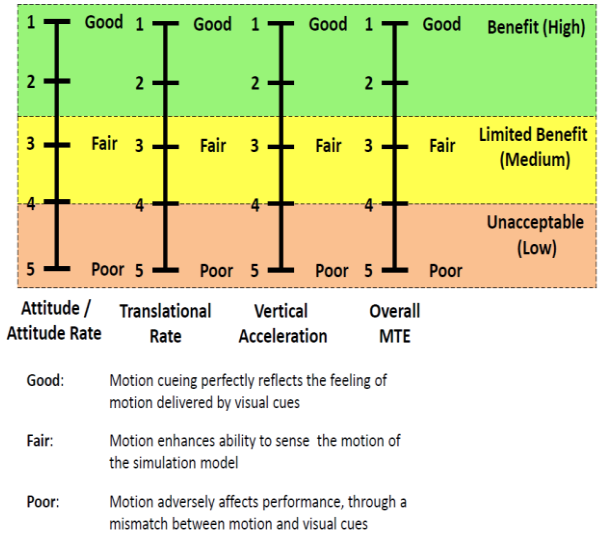

Figure 8: OMFR Scale (Ref. 18)

Superslide Task Case

The Superslide task is a land-based task aimed at representing a Shipborne Landing Flight Test Manoeuvre (FTM) (Ref. 35). The Superslide task contains elements of the station keeping requirements apparent in deck landings. In the motion cueing optimisation study, only the hover portion of the overall task was tested and examined. The hover element of the task required tracking of a moving black hover board, (see Figure 9) which is driven horizontally and vertically to replicate the motion of the ship's landing deck. In the current work it represented the motion of a frigate in a Sea State 4 condition and constitutes a pursuit tracking task where the target (i.e. the hover board) is independently moving (Ref. 1).

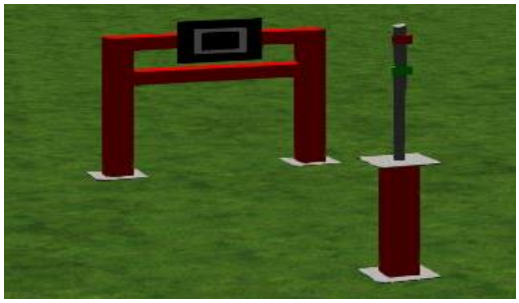

Figure 9: Superslide Course in Heliflight-R Simulator

Within the task, the dominant motion axes were roll and pitch; therefore, the motion parameter variation was undertaken in these axes only, while the parameters in the other axes remained constant. Six different MTSs and corresponding simulated aircraft accelerations sample dataset obtained during the flight trial were acquired to calculate the VMPE. These MTSs are plotted on the Sinacori chart in Figure 10, which defines the high, medium and low motion fidelity boundaries. The comparison of the results obtained from the VMPE offline test and OMFR subjective experiment is shown in Figure 11.

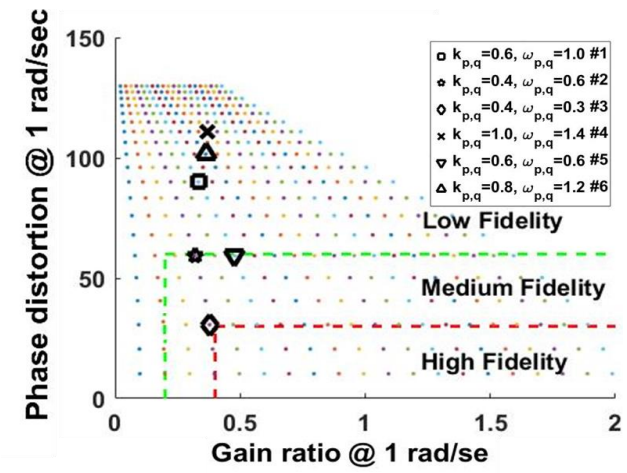

Figure 10: Sinacori Chart (Superslide)

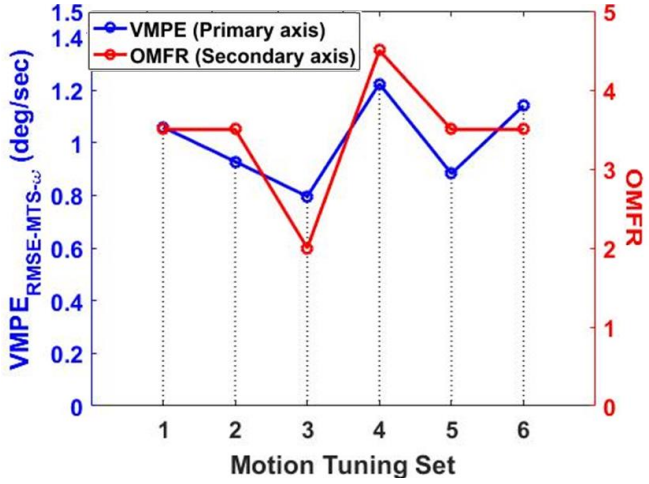

Figure 11: VMPE and OMFR Comparison (Superslide)

Comparison of the VMPE estimations with the OMFR ratings shown in Figure 11 show that the two correlate well, and that out of all the MTSs tested, MTS#3 was awarded lowest OMFR ratings and the VMPE estimated for it was minimum as well, suggesting best motion cues provided to the pilot. MTS#4 was awarded highest OMFR and the VMPE was estimated to be highest as well, suggesting this provides the worst motion cues. The Sinacori chart shows that the MTS#3 is closest to the high-fidelity region while MTS#4 is farthest in the low fidelity region, (see Figure 10).

The Lateral reposition, and Pirouette tasks were also examined using the same VMPE methodology in the pre-validation phase. A similar level of correlation between VMPE estimations and OMFR ratings was obtained in these two cases as well. From all these pre-validation exercises it was found that the VMPE estimations correlate reasonably well with the subjective ratings and the Sinacori boundaries. This provided confidence in using the VMPE technique for the offline optimisations.

The next step of the VMPE application was to derive the MTSs for a full-axis shipboard task by utilising the simulated aircraft accelerations data obtained from a previous deck landing flight trial experiment conducted using a baseline non-optimised motion configuration.

Phase II: Pre-trial Optimisation

The next stage in the process began with the acquisition of FLIGHTLAB SH-60B simulated aircraft accelerations datasets from a QEC deck landing flight trial (Ref. 30).

Three WOD airwake conditions were chosen (25, 35 and 45kts headwind ‘H00’) for the motion study. Initially, a baseline MTS was selected, and tuning was performed. The optimisation strategy was to perform a trade-off between gains ‘k’ and washout

frequencies 'ω_n' of the translational and rotational channel, with an objective of minimising the overall motion perception error (VMPE), while keeping the simulator motion constrained within platform limits. The idea was to derive new MTSs with a sufficient amount of motion perception error difference between them to test and examine the effects of different motion cueing on the performance of the deck landing operations. Four different motion tuning sets (Benign, Intermediate, Responsive and Optimised) were derived. 'Benign' MTS as its name suggests was predicted to provide the worst motion cues and 'Optimised' the best. Moreover, it was intended to further assess the correlation between the offline VMPE predictions and subjective results provided by the pilot.

Since in the deck landing operation all the axes are required for the motion cues and are relevant to the mission task, tuning was performed in all the axis (surge, sway, heave, pitch, roll, and yaw). NRMSs of the motion perception errors were calculated individually for each axis and averaged to estimate the VMPE "$VMPE_{NRMSE\text{-}MTS}$" for a complete motion tuning set using Eqn. 14.

Optimisation Results

For the optimisation, a baseline MTS was initially obtained from the generic Heliflight-R configuration and then the CWA parameters were tuned to obtain different MTSs using the VMPE technique.

Figure 12 shows the results of the estimated VMPEs for the three WOD conditions and four MTSs, for one of the flight trial datasets used for the optimisation. Pearson's correlation coefficients (ρ) between the motion perceived in the simulator and simulated aircraft for each of the twelve cases are shown in Figure 13. Correlation coefficients were estimated for each axis and averaged to provide the correlation for a MTS case.

It can be seen from Figure 12 and 13 that as VMPE decreases from 'Benign' to 'Optimised' MTS, and the correlation coefficient increases, respectively, for each of the three WOD cases. The 'Benign' motion tuning set was overall predicted to provide the worst motion cueing and 'Optimised' as the best, based on mean motion perception error (black dotted line) minimised from 9.3% to 6.1% and the mean correlation increased from 56.2% to 78.3%.

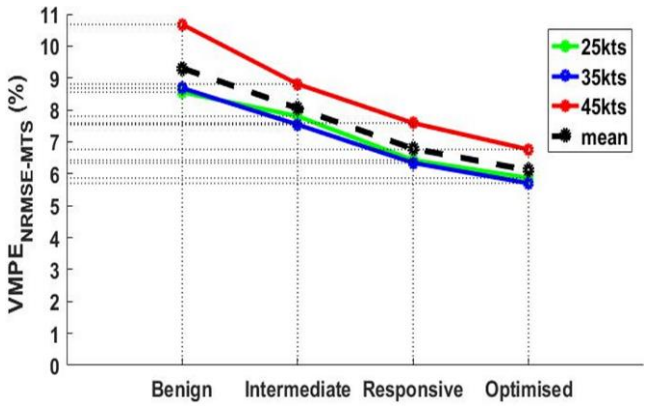

Figure 12: VMPE Results for the QEC Landing Task

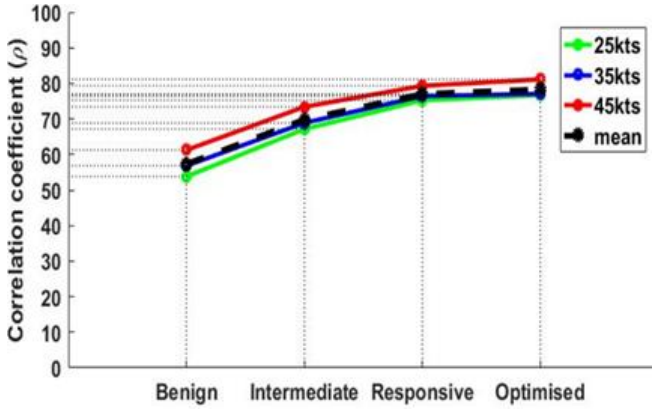

Figure 13: Correlation Coefficient between Motion Perception in Aircraft and Simulator

The Sinacori chart in Figure 14 shows the HP and LP filter parameters for the four MTSs obtained. 'Bn' is Benign, 'In' is Intermediate, 'Rp' is Responsive and 'Op' is Optimised. The chart shows the section of the high, medium and low motion fidelity regions based on the magnitude ratio and phase distortion of the washout filter used in linear and angular channels of the CWA in the frequency domain. The increase in washout filter gain values 'k' will increase the magnitude response while the increase in washout frequency 'ω_n' will decrease the magnitude response and increase phase distortion.

It can be seen that, between 'Benign' and 'Intermediate' MTS, the filter gains and washout frequencies are both increased in the pitch and roll axes while in the yaw axis and linear channels, the gains are increased, and the washout frequencies are decreased. The rationale for this was to observe the effect of the increase in the magnitude response and the phase difference between simulated aircraft and the simulator motion in pitch and roll axes on the overall motion perception. Between 'Responsive' and 'Optimised' MTSs, the gains were increased in pitch and roll axis and decreased slightly in surge and sway axis to make efficient use of the motion envelope since linear displacements demand larger simulator actuator extension, while the washout frequencies were decreased in all axis to improve the phase distortion.

Only four MTSs were derived due to the Heliflight-R motion excursion limits and the requirement to obtain sufficient VMPE estimate difference between two MTSs in order to allow the pilots to perceive noticeable motion cueing difference/mismatch. For all the tuned cases it can be observed from the Sinacori chart (Figure 14) that there was more opportunity to optimise the motion cueing in the angular channel as it would demand a less extension of the simulator actuators and hence filter values could be obtained in the high fidelity region. Due to the limits of the motion envelope translational filter values in the low fidelity region were obtained. This requirement to harmonise motions in different axes was observed in Hodge's motion experiment (Ref. 19). It is dependent on the size of the platform motion envelope and the aggressiveness of the mission task under examination.

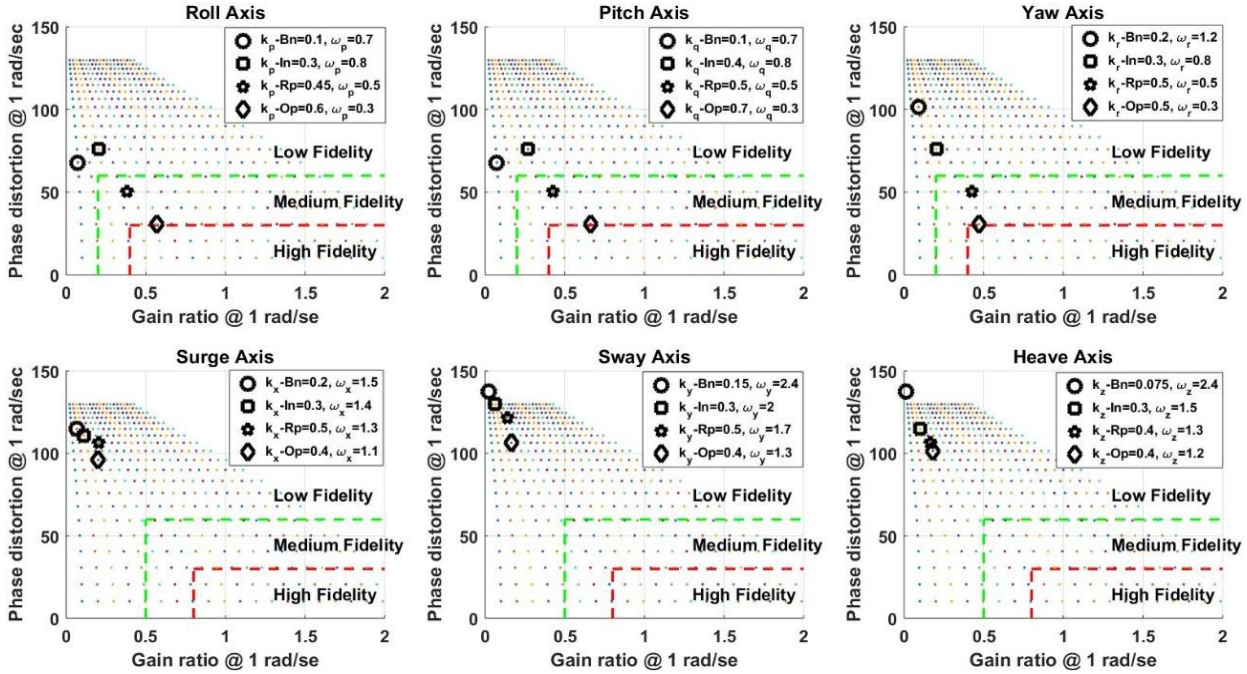

Figure 14: Four New MTSs Plotted on Sinacori Chart for Each Axis

Figures 15 and 16 shows the comparison between the perceived motion (specific forces 'f_i-per' and angular velocity 'ω_i-per') in the aircraft and simulator in all six axes obtained within the optimisation phase for the same example case for which VMPE estimations are shown in Figures 12 and 13. Simulation results from two 45kts WOD cases 'Benign' and 'Optimised' are shown, since these were assumed to provide the maximum cueing difference to the pilot; this was demonstrated by the flight trial experimental results. The grey area between the lines defines the error between the simulator and aircraft motion perception which is quantified using the RMS measure (Eqns. 8 and 9) and thus motion cueing predictions were made on basis of that. It can be seen from the plots that the grey area in the 'Benign' case is considerably larger than the 'Optimised' case. The plots also show the human motion perception threshold limits in dotted black lines acquired from a motion perception threshold detection experiment conducted in the SIMONA simulator (Ref. 36). The SIMONA limits are 0.07, 0.07, and 0.012 m/s^2 for surge, sway, and heave, respectively, and 0.0052, 0.0073, and 0.016 rad/s for pitch, roll and yaw, respectively. However, there is still some debate regarding the correct or universally accepted values of the threshold. These values are highly influenced by the simulation environment, equipment used, human subject and the task under examination. The threshold in the yaw axis is a magnitude higher than the pitch and roll axis. Recent research suggests that the yaw rate threshold plateau is 0.0126 rad/s (Ref. 37).

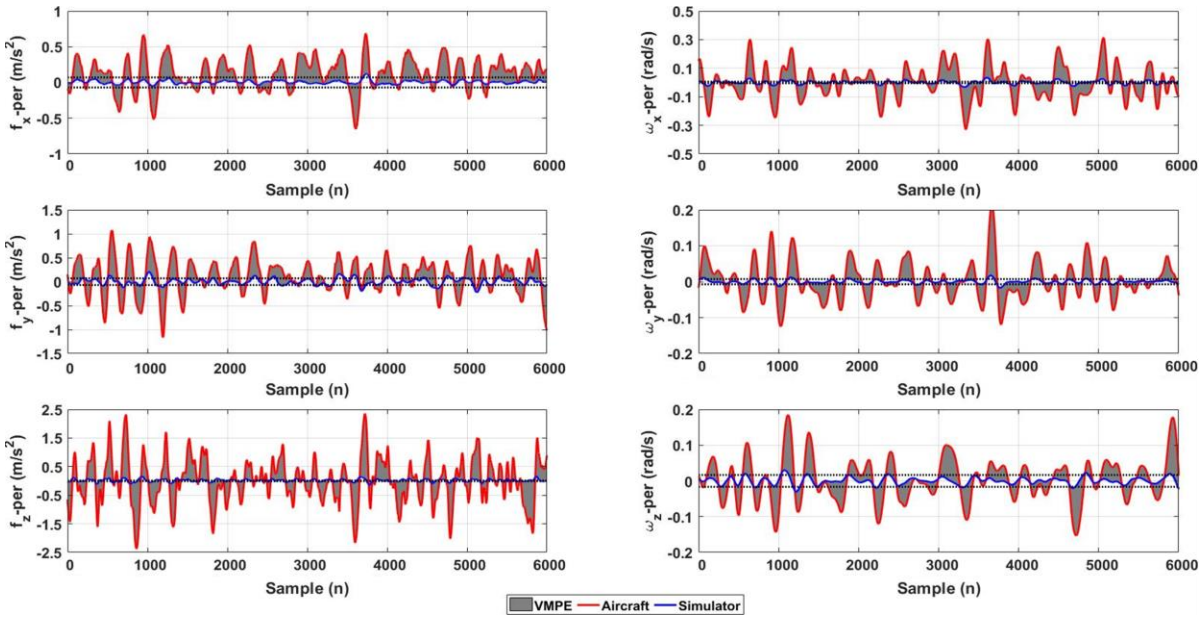

Figure 15: Comparison of Perceived Specific Forces and Angular Velocities for Benign 45kts MTS Case

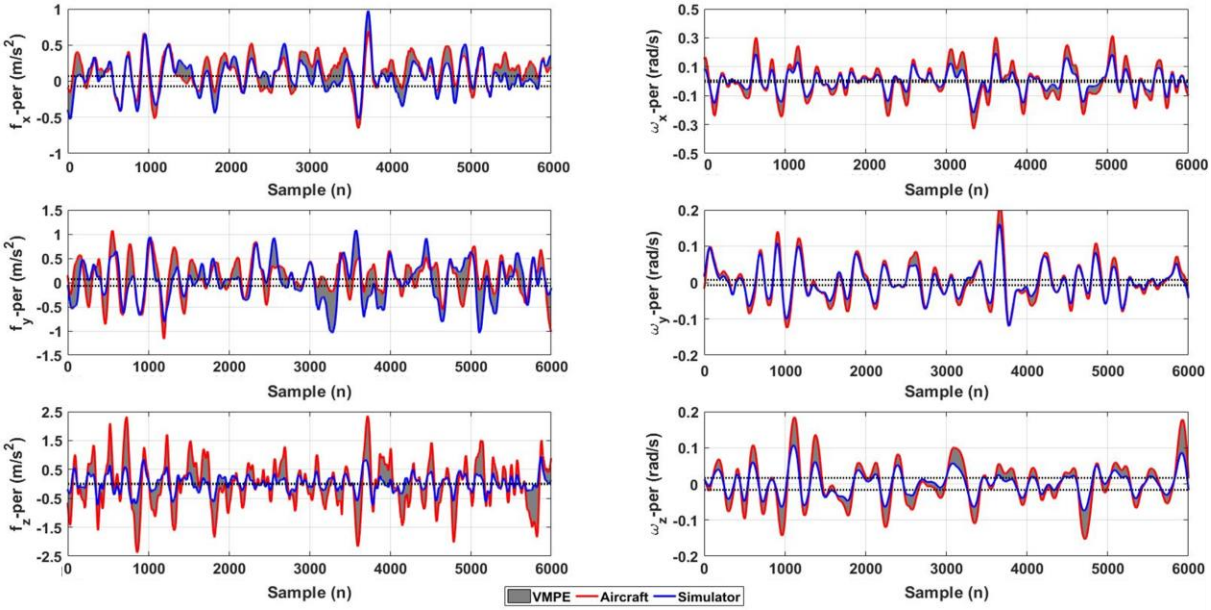

Figure 16: Comparison of Perceived Specific Forces and Angular Velocities for Optimised 45kts MTS Case

From the plots, it can be seen that, although the perception in the 'Benign' case (Figure 15) is mostly below the threshold limits except in a few instances, the pilot has still commented that he perceived physical motion during the flight trial experiment, though the motion felt was extremely gentle. The comments and subjective results are detailed in the next section. This observation suggests that further research is required to determine more representative motion perception threshold limits specifically for simulated operations in HSDI environments.

Phase III: Flight Trial Experiment

Once the new MTSs were derived, the next step was to conduct a flight trial experiment to examine the motion cueing fidelity. A piloted flight simulation trial was conducted by an experienced ex-Royal Navy pilot consisting of a test matrix of twelve QEC deck landings on Spot-5 (Shown in Figure 17) at three WOD conditions using the four new MTSs.

The pilot was initially briefed about the Mission Task Elements (MTEs) and that he would experience a range of the different motion cues in a random order. The landing procedure was split into three MTEs as shown in Figure 17. MTE 1 consists of a lateral translation across the flight-deck to a position above the landing spot, at a hover height of 30ft. MTE 2 consists of a 30 second period of stabilized hover station-keeping prior to the landing. Finally, MTE 3 is the descent from the hover to touchdown on the flight deck.

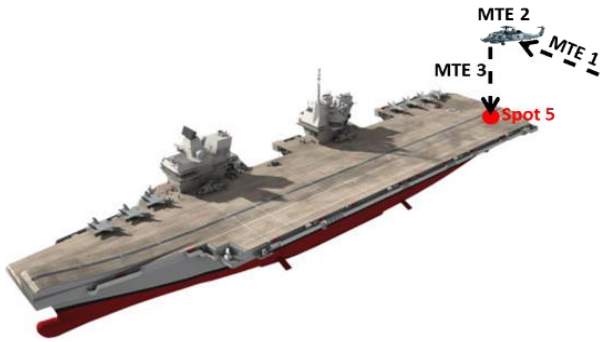

Figure 17: QEC Deck Landing Task to Spot 5

The motion fidelity was assessed and rated subjectively using the Hodge Motion Fidelity Rating Scale (HMFR) (Figure 18), proposed by Hodge et al. (Ref. 17). The rating scale is a 10-point scale which has the same structure as that of the Cooper-Harper Handling Quality Rating (HQR) scale.

FLIGHT TRIAL RESULTS

Figure 19 shows the flights trial results for the twelve cases tested. The coloured region specifies the decision tree regions from the HMFR scale shown in Figure 18. An overall agreement was obtained between offline VMPE predictions and piloted simulation HMFR results. The 'Benign' motion set was subjectively rated worst and 'Optimised' as best by the pilot, as predicted during the offline optimisation using VMPE technique. The prediction was true for 'Intermediate' and 'Responsive' MTSs also.

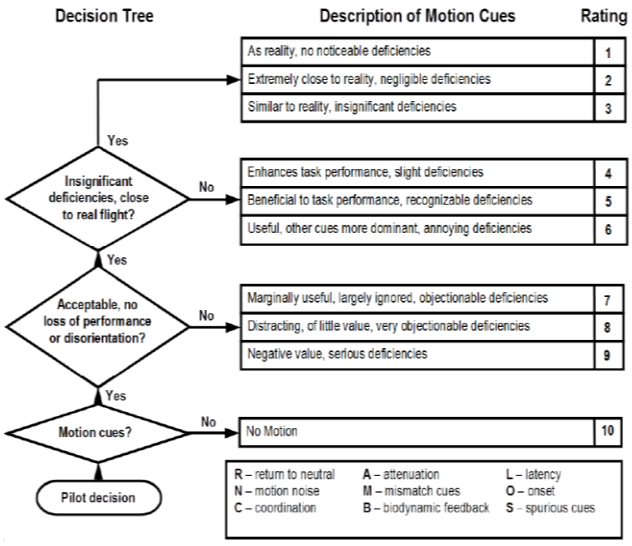

Figure 18: Hodge Motion Fidelity (HMFR) Scale

It can be seen from Figure 19 that at 25kts WOD condition the subjective ratings remained constant overall for all the MTSs, this is possibly due to the reason that at this WOD condition the motion cues obtained from the visual scene (i.e. vection) are sufficient for the pilot performing the task in a low turbulent environment. This was later confirmed from pilot comments, where pilot at 25kts case has commented that "Hardly any airwake felt (gentle disturbance)", "felt very little physical motion" and "No changes in displacement due to low WOD wake".

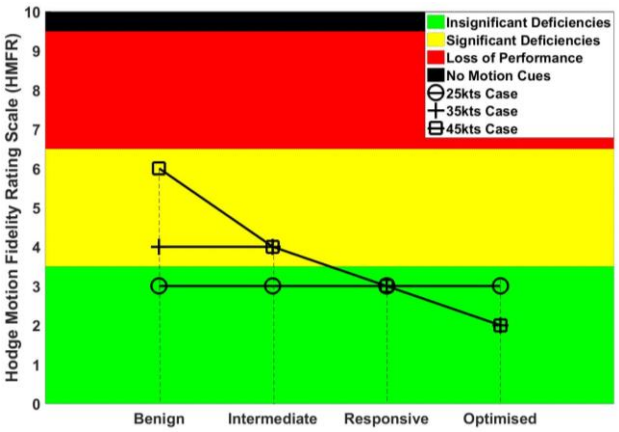

Figure 19: Flight Trial Experiment Subjective Results

However, when the WOD condition was increased to 35kts and 45kts using the 'Benign' MTS the HMFR increases to 4 and 6 suggesting slight and annoying motion cueing deficiencies, respectively. The pilot has then commented that "Poor cueing in hover", "little touch down felt", "significant visual/vestibular mismatch" and "Pilot would expect to bounce around at this WOD condition". The HMFR decreases to 2, at same WOD conditions using the 'Optimised' MTS, suggesting good motion cueing experience with negligible deficiencies. The pilot commented "Feeling airwake in all axes", "visual and physical feeling of motion is realistic and in sync", "felt vertical bouncing" and "pilot could both feel and see displacements".

Figure 20 shows the aircraft trajectories for the two extreme cases, 45kts 'Benign' MTS rated HMFR=6 and 45kts 'Optimised' MTS rated HMFR=2. An expanded view of the trajectories of the hover MTE is presented in the boxes. It can be seen that the spatial deviation from the hover station-keeping point in the 45kts 'Benign' MTS case (blue line) is larger than the 45kts 'Optimised' MTS case (red line). This deviation in the 'Benign' case is possibly a result of the degraded motion cues which have led to the loss of task performance where the pilot has commented "Poor activity on the controls" and "Poor motion cueing in hover". Whereas in the 'Optimised' case more representative motion cues were provided resulting in better task performance where the pilot has commented "Relatively accurate controls with small inputs". These observations were further supported by analysing the pilot control stick inputs.

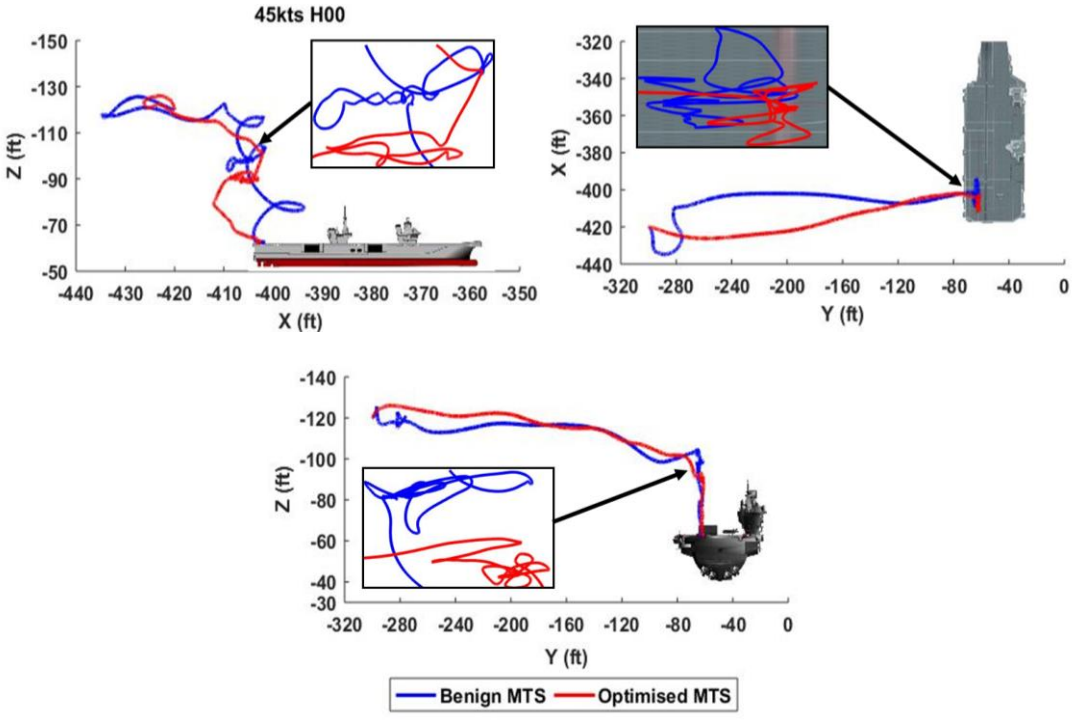

Figure 20: Flight Trial QEC Deck Landing Trajectory

Figure 21 shows the control activity of the pilot for the same two extreme cases in the hover MTE only. The pilot stick movement in the 'Benign' MTS case while station-keeping is noticeably larger than the 'Optimised' MTS case at same WOD condition. This is due to poor vestibular motion cues available to the pilot, which hampers the overall simulation fidelity due to a larger mismatch between visual and vestibular motion cues. This observation was supported by pilot comments detailed previously. The lateral control input range came within 16.75% in 'Benign' MTS and 7.9% in 'Optimised' MTS, and longitudinal control input in 14.7% in 'Benign' and 8.0% in 'Optimised', respectively. Thus, it shows that the motion cues has influenced the control activity of the pilot.

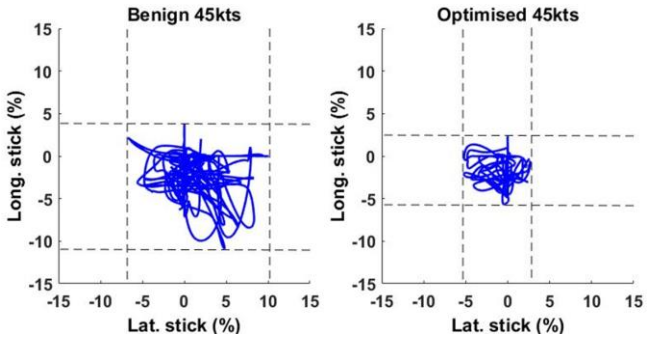

Figure 21: Pilot Cyclic Control Activity in Hover MTE

To further analyse the effect of the motion cues, Figure 22 shows the frequency analysis comparing the simulator and aircraft actual specific forces and angular rates obtained at the pilot VC. The results are shown for the actual specific force 'f_{sp}_x' in x-axis and pitch rate 'ω_{sp}_y' only, since these are the dominant axes for the H00 airwake condition experienced by the pilot in hover. When using 'Benign' MTS the simulator response is compromised resulting in loss of the peaks of the amplitude throughout the frequency range. While in the 'Optimised' MTS the simulator seems to reproduce the response reasonably well throughout the frequency range. This suggests that when using the 'Benign' MTS, the simulator is not able to provide sufficient airwake turbulence feedback to the pilot via vestibular motion cues. Whereas in the 'Optimised' MTS the pilot would perceive more representative motion cues and airwake turbulence feedback due to better reproduction of the aircraft accelerations by the simulator's motion platform. The results are supported by the pilot comments and HMFR ratings along with the comparison of the pilot control activity detailed in the previous section for the same two extreme cases. Note the amplitude of FFT is normalized by the signal length to change the scale to the true amplitude.

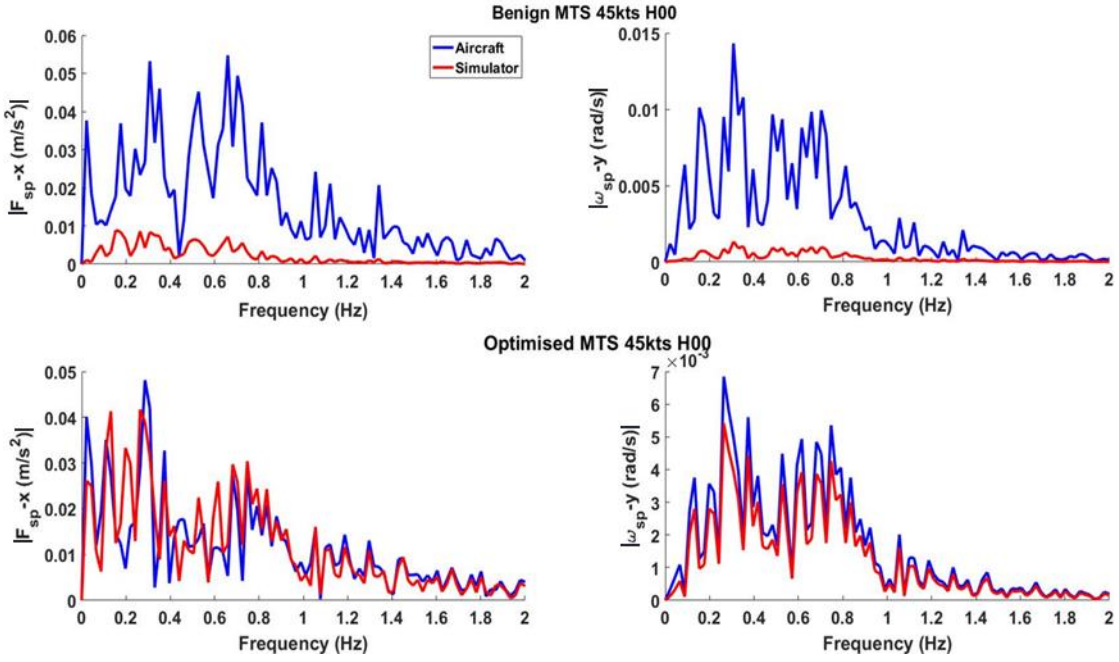

Figure 22: Frequency Domain Comparison of Actual Specific Forces and Angular Rates in Benign and Optimised MTS

CONCLUSIONS AND FUTURE WORK

The research presented in this paper details initial progress in establishing motion fidelity requirements for simulated HSDI operations which improve the overall fidelity of the maritime rotorcraft simulators used to inform and support FOCFT. Thepaper has presented the results for the assessment and optimisation of the vestibular motion cues within the Heliflight-R rotorcraft simulator for the QEC deck landing operations. A new motion optimisation technique 'VMPE' has been introduced in this study and used to develop new motion tuning sets for use in a pilot simulated flight trial. An overall agreement was obtained between the VMPE predictions and flight trial results.

It was found that the "high-fidelity" motion cueing becomes more desirable at higher airwake wind conditions than at lower winds, due to higher perturbations in the airflow over and around the ship's landing deck and the subsequent disturbance of the helicopter. Pilot HMFR ratings at 25kts WOD condition remained the same (i.e. HMFR 3-3-3-3) when flying the simulator with any of the four motion tuning sets. However, when the WOD airwake condition was increased to 35kts and 45kts, the motion cueing for the pilot flying the simulator with 'Benign' motion set degrades (i.e. HMFR 4-6), while it gets more representative (better) with 'Optimised' motion set (i.e. HMFR 2-2).

The results from the flight trial experiment for the two extreme cases (45kts 'Benign' HMFR=6 and 45kts 'Optimised' MTS HMFR=2), indicated that motion cueing influenced the task performance and the control activity of the pilot. The representative and synchronised motion cues helped the pilot to perform the task satisfactorily due to the smallest mismatch between vestibular and visual motion cues hence a better overall self-motion perception. The 'Optimised' MTS gave the lowest HMFR ratings for the WOD conditions tested, therefore, it can be regarded as a universal motion setting for the lower as well as higher airwake conditions, at least for the simulated operations on the QEC aircraft carrier.

The VMPE technique can be used for motion assessment and optimisation for a particular task and provides a means of characterising motion perception in the aircraft and simulator. It can be used to derive task-specific motion tuning sets and for use in simulation trials prior to real-world testing.

The benefit of the motion tuning technique has yet to be fully demonstrated. The methodology presented here, and the MTSs examined, have not been tested for a range of ships and HSDI conditions, this will be examined in an upcoming motion-dedicated flight trial experiment. Testing of this methodology with simulators with larger motion envelopes will help establish the motion fidelity requirements for maritime simulators; this will be pursued in future work.

Author contact:
Wajih Memon wajih.ahmed.memon@liverpool.ac.uk, Mark D White mdw@liverpool.ac.uk and Ieuan Owen i.owen@liverpool.ac.uk.

ACKNOWLEDGEMENTS

The lead author would like to thank: Dr Michael Jones from the DLR, for providing access to the ADS-33 experimental data he obtained during the piloted simulation flight trial experiment conducted at the University of Liverpool; Michael Francis Kelly, a PhD Student at the University of Liverpool, for access to the QEC airwake data used for the flight trial; and Andy Berryman, an ex-RN pilot, who conducted the simulation flight trials.

REFERENCES

[1]Lumsden, B., and Padfield, G. D., "Challenges at the Helicopter-Ship Dynamic Interface," 24th European Rotorcraft Forum Proceedings, Marseilles, France, September 15-17, 1998.

[2]Fang, R., Krijns, H. W., and Finch, R. S., "Dutch/British Clearance Process," RTO AGARDograph 300: Helicopter/Ship Qualification Testing, Vol. 22, Flight Test Techniques Series, NATO Research and Technology Organization, 2003.

[3]Forrest, J. S., Owen, I., Padfield, G. D., and Hodge, S. J., "Ship-Helicopter Operating Limits Prediction Using Piloted Flight Simulation and Time-Accurate Airwakes," *Journal of Aircraft*, Vol. 49, (4), June. 2012, pp. 1020-1031.

[4]Advani, S., and Wilkinson, C., "Dynamic Interface Modelling and Simulation - A Unique Challenge," Royal Aeronautical Society Conference on Helicopter Flight Simulation Proceedings, London, November 2001.

[5]Roscoe, M. F., and Wilkinson, C. H., "DIMSS - JSHIP's M&S Process for Ship helicopter Testing and Training," AIAA Modelling and Simulation Technologies Conference and Exhibit Proceedings, California, USA, August 5-8, 2002.

[6]Val, J., and Healey, V., "Simulating the Helicopter-Ship Interface as an Alternative to Current Methods of Determining the Safe Operating Envelopes," NAVAIR: Air Vehicle Division, 1986.

[7]Hodge, S., Padfield, G. D., and Southworth, M. R., "Helicopter-Ship Dynamic Interface Simulation: Fidelity at Low-Cost," RAeS Cutting Costs in Flight Simulation–Balancing Quality and Capability Proceedings, London, UK, November 2006.

[8]Owen, I., White, M. D., Padfield, G, D., and Hodge, S., "A Virtual Engineering Approach to the Ship-Helicopter Dynamic Interface; A Decade of Modelling and Simulation Research at the University of Liverpool," *The Aeronautical Journal*, Vol. 49, (1246), December. 2017, pp. 1833-1857.

[9]Wang, Y., White, M. D., Owen, I., Hodge, S., and Barakos, G., "Effects of visual and motion cues in flight simulation of ship borne helicopter operations," 38th European Rotorcraft Forum Proceedings, Amsterdam, September 4-7, 2012.

[10]Perfect, P., Timson, E., White, M. D., Padfield, G. D., Erdos, R., and Gubbels, A. W., "A Rating Scale for the Subjective Assessment of Simulation Fidelity," *The Aeronautical Journal*, Vol. 11, (1206), August. 2014, pp. 953–974.

[11]Perfect, P., White, M. D., Padfield, G. D., and Gubbels, A. W., "Rotorcraft Simulation Fidelity: New Methods for Quantification and Assessment," *The Aeronautical Journal*, Vol. 117, (1189), March. 2013, pp. 235-282.

[12]EASA. "European Aviation Safety Agency Certification Specifications for Helicopter Flight Simulation Training Devices," 'CS-FSTD (H)', 2012.

[13]FAA. "Flight Simulation Training Device Initial and Continuing Qualification and Use," '14 CFR Part 60', 2016, https://www.faa.gov/about/initiatives/nsp/media/14cfr60_se archable_version.pdf.

[14]Timson, E., Perfect, P., White, M. D., Padfield, G. D., Erdos, R., and Gubbels, A., W., "Subjective Fidelity Assessment of Rotorcraft Flight Training Simulators," American Helicopter Society 68th Annual Forum Proceedings, Fort Worth, TX, USA, May 2012.

[15]Pavel, M. D., White, M. D., Padfield, G. D., Roth, G., Hamers, M., and Taghizad, A., "Validation of Mathematical Models for Helicopter Flight Simulators Current and Future Challenges," *The Aeronautical Journal*, Royal Aeronautical Society, Vol. 117, (1190), April. 2013, pp. 343–388.

[16]White, M. D., Perfect, P., Padfield, G. D., Gubbels, A. W., and Berryman, A. C., "Acceptance Testing And Commissioning of a Flight Simulator for Rotorcraft Simulation Fidelity Research," *Institution of Mechanical Engineers, Part G: Journal of Aerospace Engineering*, Vol. 227, (4), June. 2012, pp. 663–686.

[17]Manso, S., White, M. D., and Hodge, S., "An Investigation of Task-Specific Motion Cues for Rotorcraft Simulators," In AIAA Modelling and Simulation Technologies Conference Proceedings, San Diego, California, Jan 4-8, 2016.

[18]Jones, M., White, M. D., Fell, T., and Barnett, M., "Analysis of Motion Parameter Variations for Rotorcraft Flight Simulators," American Helicopter Society 73rd Annual Forum Proceedings, Fort Worth, Texas, USA, May 9-11, 2017.

[19]Hodge, S. J., "Dynamic Interface Modelling and Simulation Fidelity Criteria," Doctoral Thesis, University of Liverpool, September 2010.

[20]Hodge, S. J., Perfect, P., Padfield, G. D., and White, M. D., "Optimising The Roll-Sway Motion Cues Available From A Short Stroke Hexapod Motion Platform," *The Aeronautical Journal*, Vol. 119, (1211), January. 2015, pp. 23-44.

[21]Hosman, R. J. A. W., Cardullo, F. M., and Bos, J. E., "Visual-Vestibular Interaction in Motion Perception," AIAA Modelling and Simulation Technologies Conference Proceedings, Oregon, August 08-11, 2011.

[22]Nash, C. J., Cole, D. J., and Bigler, R. S., "A Review of Human Sensory Dynamics for Application to Models of Driver Steering," *Biol. Cybern*, Vol. 110, 2016, pp. 91–116.

[23]Grundy, J. G., Nazar, S., Omalley, S., Mohrenshildt, M. V., and Shedden, J. M., "The Effectiveness of Simulator Motion in the Transfer of Performance on a Tracking Task is Influenced by Vision and Motion Disturbance Cues," *Human Factors*, Vol. 58, (4), June. 2016, pp. 546–559.

[24]Reid, L., and Nahon, M., "Flight Simulation Motion-Base Drive Algorithm: Part1-Developing and Testing the Equations," UTIAS Report No.296, December 1985.

[25]Nehaoua, L., Mohellebi, H. Amouri, A., Arioui, H. Espié, S., and Kheddar, A., "Design and Control of a Small-Clearance Driving Simulator," *IEEE Transactions on Vehicular Technology*, Vol. 57, (2), March. 2008, pp. 736-746.

[26]Casas, S., Coma, I., Portales, C., and Fernandez M., "Towards a Simulation-Based Tuning of Motion Cueing Algorithms," *Simulation Modelling Practice and Theory*, Vol. 67, September 2016, pp. 137–154.

[27]Asadi, H., Mohamed, S., Zadeh, D. R., and Nahavandi, S., "Optimisation of Nonlinear Motion Cueing Algorithm Based on Genetic Algorithm," *Vehicle system dynamics*, Vol. 53, (4), December 2015, pp. 526-545

[28]Jones, M., "Enhancing Motion Cueing Using an Optimisation Technique," *The Aeronautical Journal*, Vol. 122, March 2018, pp. 487-518.

[29]White, M. D., Dadswell, C. Fell, T., and Coates, R., "The Use of Modelling and Simulation to Give Students a HEADSTART into Aerospace Engineering," AIAA Modelling and Simulation Technologies Conference Proceedings, AIAA SciTech Forum, Grapevine, Texas, USA, January 9-13, 2017.

[30]Kelly, M. F., White, M. D., Owen, I., and Hodge, S. J., "Piloted Flight Simulation for Helicopter Operation to the Queen Elizabeth Class Aircraft Carriers," 43rd European Rotorcraft Forum Proceedings, Milan, Italy, September 12-15, 2016.

[31]Sinacori, J. B., *"*A Practical Approach to Motion Simulation*,"* A1AA Visual and Motion Simulation Conference Proceedings, AIAA Paper No. 73-931, Palo Alto, California, September 10-12, 1973.

[32]Plemenos, D., and Miaoulis, G., *Intelligent Computer Graphics*, Springer-Verlag Berlin Heidelberg, 2010, pp. 153.

[33]Shcherbakov, M. V., Brebels, A., Shcherbakova, N. L., Tyukov, A. P., Janovsky, T. A., and Kamaev, V. A., "A Survey of Forecast Error Measures," *World Applied Sciences Journal (Information Technologies in Modern Industry, Education & Society)*, Vol. 24, September. 2013, pp. 171-176.

[34]Anon., "Aeronautical Design Standard Performance Specification Handling Qualities Requirements for Military Rotorcraft," ADS-33E-PRF, United States Army Aviation and Missile Command, Redstone Arsenal, AL, 2000.

[35]Carignan, S., Gubbels, A., and Ellis, K., "Assessment of Handling Qualities for the Shipborne Recovery Task - ADS 33 (Maritime)," 56th American Helicopter Society Annual Forum Proceedings, Virginia Beach, VA, May 1-4, 2000.

[36]Heerspink, H. M., Berkouwer, W. R., Stroosma, O., Paassen, M. M., Mulder, M., and Mulder, J. A., "Evaluation of Vestibular Thresholds for Motion Detection in the SIMONA Research Simulator," AIAA Modeling and Simulation Technologies Conference and Exhibit Proceedings, San Francisco, California, August 15-18, 2005.

[37]Soyka, F., Giordano, P. R., Barnett-Cowan, M., and Bülthoff, H. H., "Modeling Direction Discrimination Thresholds for Yaw Rotations around an Earth-Vertical Axis for Arbitrary Motion Profiles," *Experimental Brain Research*, Vol. (220), (1), July. 2012, pp. 89-99.